[*Supporting Information*]

Thioether-Based Fluorescent Covalent Organic Framework for Selective Detection and Facile Removal of Mercury(II)

San-Yuan Ding,[†] Ming Dong,[†] Ya-Wen Wang,[†] Yan-Tao Chen,[†] Huai-Zhen Wang,[†] Cheng-Yong Su,[‡] and Wei Wang*[,†,§]

[†] *State Key Laboratory of Applied Organic Chemistry, College of Chemistry and Chemical Engineering, Lanzhou University, Lanzhou, Gansu 730000, China;*

[‡] *School of Chemistry and Chemical Engineering, Sun Yat-Sen University, Guangzhou 510275, China*

[§] *Collaborative Innovation Center of Chemical Science and Engineering, Tianjin 300071, China*

* E-mail: wang_wei@lzu.edu.cn

A. Summary of Figures and Tables

B. General Information

Materials

All reagents, unless otherwise noted, were purchased from commercial sources and used without further purification. Dioxane, acetone, acetonitrile, and acetic acid were purified through the standard procedures.

Instrumentation

Liquid ^{1}H and ^{13}C NMR spectra were collected on a Bruker Avance III 400 MHz NMR spectrometer using tetramethylsilane (TMS) as an internal standard.

Elemental analysis was carried out on an Elementar Analysensysteme GmbH VarioEL V3.00 elemental analyzer.

FT-IR spectra were recorded with a Nicolet NEXUS 670 instrument.

Powder X-ray diffraction (PXRD) data were collected with a PANalytical X'Pert Pro diffractometer operated at 40 kV and 40 mA with Cu Kα radiation (step size: 0.017^{o}, step time: 10.34 s).

Solid-state NMR experiments were performed on a Bruker WB Avance II 400 MHz NMR spectrometer. The ^{13}C CP/MAS NMR spectra were recorded with a 4-mm double-resonance MAS probe and with a sample spinning rate of 10.0 kHz; a contact time of 2 ms (ramp 100) and a pulse delay of 3 s were applied.

The nitrogen adsorption and desorption isotherms were measured at 77 K using a Micromeritics ASAP 2020M system. The samples were outgassed at 120 ^{o}C for 8 h before the measurements. Surface areas were calculated from the adsorption data using Langmuir and Brunauer-Emmett-Teller (BET) methods, respectively. The pore-size-distribution curves were obtained via the non-local density functional theory (NLDFT) and the Barrett-Joyner-Halenda (BJH) method.

Field emission scanning electron microscopy (SEM) observations were performed on a Hitachi S-4800 microscope operated at an accelerating voltage of 5.0 kV.

The thermal properties of COF-LZU8 material were evaluated using a STA PT1600 Linseis thermogravimetric analysis (TGA) instrument over the temperature range of 25 to 800 °C under nitrogen atmosphere with a heating rate of 10 °C/min.

X-ray photoelectron spectroscopy (XPS) data were obtained with an ESCALab210 VG Scientific electron spectrometer using 300 W Mg Kα radiation. The binding energies were referenced to the C_{1s} line at 285.0 eV from the adventitious carbon.

The mercury contents were determined by inductively coupled plasma (ICP) analysis with an IRIS Advantage instrument. The trace contents of mercury were determined with an AFS-9800 atomic fluorescence spectrometer.

Fluorescence spectra were recorded at room temperature using a Hitachi F-7000 spectrophotometer with a PMT voltage of 700 V and a scan speed of 1200 nm/min; the slit width for both excitation and emission was 5 nm. The time-dependent fluorescence spectra (Figure S5) recorded for COF-LZU8 dispersed in acetonitrile indicated that COF-LZU8 does not show any photo-bleaching. The fluorescent quantum yields were measured on an FLS920 spectrometer from Edinburgh Instruments, using the method[1] for measuring the absolute photoluminescence quantum yield.

Stock solutions (1.0 mM) of the perchlorate salts of Hg^{2+}, Li^{+}, Na^{+}, K^{+}, Ag^{+}, Mg^{2+}, Ca^{2+}, Ba^{2+}, Al^{3+}, Pb^{2+}, Cu^{2+}, Fe^{2+}, Fe^{3+}, Co^{2+}, Ni^{2+}, Zn^{2+}, Sr^{2+}, and Cd^{2+} were prepared in ethanol; and the stock solutions (1.0 mM) of S^{2-} was prepared in deionized water using Na_2S. Stock solution of COF-LZU8 (0.3 mg/mL) was prepared by dispersion[2] of COF-LZU8 in acetonitrile. The uniformly dispersed COF-LZU8 has the average particle size of ~250 nm as demonstrated by the SEM images (Figure S17).

For the sensing (sensitivity and selectivity) tests,[2] 30 μL of the stock solution of COF-LZU8 was diluted with 3 mL of acetonitrile in a quartz cuvette. COF-LZU8 was readily dispersed in acetonitrile and the obtained suspension was almost transparent. The fluorescence spectra were recorded immediately after an appropriate aliquot of the stock solution of metal ions was added. Each test was repeated at least for three times to get concordant values. All the measurements, unless otherwise noted, were excited at λ_{ex} = 390 nm and the corresponding emission wavelength was tested from λ_{em} = 410 to 680 nm. The shape of the emission spectra was not changed upon the addition of the stock solutions of metal ions. The fluorescence titrations were carried

out via gradually adding the stock solution of Hg^{2+} in an incremental fashion. Other metal ions (2 equiv.), including Li^{+}, Na^{+}, K^{+}, Ag^{+}, Mg^{2+}, Ca^{2+}, Ba^{2+}, Al^{3+}, Pb^{2+}, Cu^{2+}, Fe^{2+}, Fe^{3+}, Co^{2+}, Ni^{2+}, Zn^{2+}, Sr^{2+}, and Cd^{2+}, were used to investigate the selectivity of COF-LZU8 toward the Hg^{2+} detection. For the recycle tests, 30 μL of the stock solution of COF-LZU8 was diluted with 3 mL of acetonitrile in a quartz cuvette, the fluorescence spectra were measured before and after the stock Hg^{2+} solution (33.3 μmol) was added. The stock solution of S^{2-} was further added[3] to remove Hg^{2+} from Hg/COF-LZU8, and the recycled COF-LZU8 was reused in the next Hg^{2+} detection and removal (see Figure S15). The measured fluorescence intensities were used to assess the degree of the recovery.

C. Synthetic Procedures

Synthesis of 2,5-bis(3-(ethylthio)propoxy)terephthalohydrazide (1).

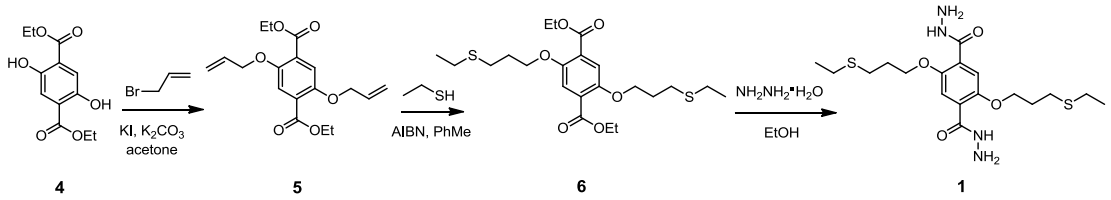

Diethyl 2,5-bis(allyloxy)terephthalate (**5**). **5** was synthesized according to the reported literature[4] with a modified procedure. 2.00 g (7.8 mmol) of diethyl 2,5-dihydroxyterephthalate (**4**) were dissolved in 150 mL of acetone, to which 9.0 g of potassium carbonate and 160 mg of potassium iodide were added. To the mixture, 3.7 mL of allyl bromide were additionally added and heated to reflux for 40 h. The mixture was hot filtered and the solid residue was washed with acetone. The yellow filtrate was then evaporated to dryness. The obtained residue was suspended in water (20 mL) and extracted with 3 × 50 mL of methylene chloride. The organic extracts were combined, washed with water and brine, and dried over with anhydrous sodium sulfate. The dried solution was then evaporated to obtain the crude product as yellow solid, which was purified by flash chromatographic column (petroleum ether/ethyl acetate: 10/1) to afford **5** (2.47 g, 95% yield). **^{1}H NMR** (400 MHz, $CDCl_3$): δ = 7.38 (s, 2H), 6.10−6.01 (m, 2H), 5.51−5.45 (m, 2H), 5.29−5.27 (m, 2H), 4.60−4.58 (m, 4H), 4.41−4.34 (m, 4H), 1.38 (t, J = 8.0 Hz, 6H). **^{13}C NMR** (100 MHz, $CDCl_3$): δ = 165.6, 151.5, 132.7, 125.0, 117.5, 117.4, 70.6, 61.3, 14.2.

Diethyl 2,5-bis(3-(ethylthio)propoxy)terephthalate (**6**). 0.5 g (1.5 mmol) of **5** and azodiisobutyronitrile (AIBN) (3.0 mmol, 0.49 g) were weighed into a glass ampoule (volume of *ca.* 20 mL, body length of 18 cm, neck length of 9 cm). The ampoule was evacuated on a vacuum line for 10 min and then injected with argon gas. To the ampoule was added toluene (1.0 mL) and ethanethiol (15.0 mmol, 1.07 mL). Then the ampoule was flash frozen in a liquid nitrogen bath, evacuated to an internal pressure of 0 mbar and flame sealed, reducing the total length by *ca.* 10 cm. Upon warming to

room temperature, the ampoule was placed in an oven at 80 ºC for 24 hours. Upon cooling down, the ampoule was broken at the neck, and the reaction mixture was evaporated to obtain the crude product as a yellow solid. The crude product was then purified by flash chromatographic column (ethyl acetate) to afford **6** (0.68 g, 98% yield). **^{1}H NMR** (400 MHz, $CDCl_3$): δ = 7.36 (s, 2H), 4.38−4.32 (m, 4H), 4.11 (t, *J* = 6.0 Hz, 4H), 2.74 (t, *J* = 7.2 Hz, 4H), 2.55−2.50 (m, 4H), 2.10−2.03 (m, 4H), 1.37 (t, *J* = 7.2 Hz, 6H), 1.24 (t, *J* = 7.2 Hz, 6H). **^{13}C NMR** (100 MHz, $CDCl_3$): δ = 165.5, 151.4, 124.5, 116.4, 67.8, 61.0, 29.0, 27.7, 25.7, 14.5, 14.1. **ESI-HRMS**: calcd. for [$C_{22}H_{34}O_6S_2$ + H] 459.1797, found 459.1868.

2,5-Bis(3-(ethylthio)propoxy)terephthalohydrazide (**1**). 1.00 g (2.2 mmol) of **6** was dissolved in 45 mL of ethanol and 6 mL of hydrazine hydrate. The mixture was stirred and heated to reflux for 12 h. After cooling, white crystals precipitated, which were isolated by filtration, and washed thoroughly with water and ethanol. The white solid was then dried to obtain the final product of **1** (0.76 g, 80% yield). **^{1}H NMR** (400 MHz, DMSO-d_6): δ = 9.23 (s, 2H), 7.32 (s, 2H), 4.57 (s, 4H), 4.11 (t, *J* = 6.0 Hz, 4H), 2.64 (t, *J* = 7.2 Hz, 4H), 2.54−2.49 (m, 4H), 2.01−1.95 (m, 4H), 1.17 (t, *J* = 7.2 Hz, 6H). **^{13}C NMR** (100 MHz, DMSO-d_6): δ = 173.8, 159.5, 135.3, 124.6, 77.8, 38.6, 37.1, 34.8, 24.6. **ESI-HRMS**: calcd. for [$C_{18}H_{30}N_4O_4S_2$ + H] 431.1781, found 431.1175.

Synthesis of 1,3,5-triformylbenzene (2).

Compound **2** was synthesized according to the reported procedure.[5] The obtained ^{1}H and ^{13}C NMR spectra of **2** matched well with those reported[5] previously.

Synthesis of COF-LZU8.

2,5-Bis(3-(ethylthio)propoxy)terephthalohydrazide **1** (65 mg, 0.15 mmol) and 1,3,5-trisformylbenzene **2** (16 mg, 0.10 mmol) were weighed into a glass ampoule (volume of *ca.* 20 mL, body length of 18 cm, neck length of 9 cm). To the mixture was added 1,4-dioxane (1.0 mL), mesitylene (3.0 mL), and 0.4 mL of 6.0 mol/L aqueous acetic acid. Then the ampoule was flash frozen in a liquid nitrogen bath, evacuated to an internal pressure of 0 mbar and flame sealed, reducing the total length by *ca.* 10 cm. Upon warming to room temperature, the ampoule was placed in an oven at 120 ºC and left undisturbed for 3 days, yielding a white solid. The ampoule was broken at the neck, and the white solid was isolated by centrifugation and washed with acetone (3 × 10 mL) and THF (3 × 10 mL), dried at 80 ºC under vacuum for 12 h to yield COF-LZU8 as a white powder (61 mg, 80% yield). COF-LZU8 could also be successfully synthesized with high crystallinity under other conditions, such as in 1,4-dioxane [1,4-dioxane/mesitylene/HOAc (6.0 M) = 15/30/2] and in ethanol [EtOH/mesitylene/HOAc (6.0 M) = 15/30/2] (see Figure S17). **Anal. Cald** for $(C_{12}H_{14}N_2O_2S)_n$: C 57.60; H 5.60; N 11.20, S 12.80. Found: C 56.72; H 5.84; N 10.72, S 12.47. **IR** (powder, cm^{-1}) 3440, 3287, 2962, 2927, 1677, 1621, 1533, 1487, 1442, 1413, 1218, 1079, 1019, 806, 569. The characterization details of COF-LZU8 are presented in the main text and in this Supporting Information.

Synthesis of the model compound 3.

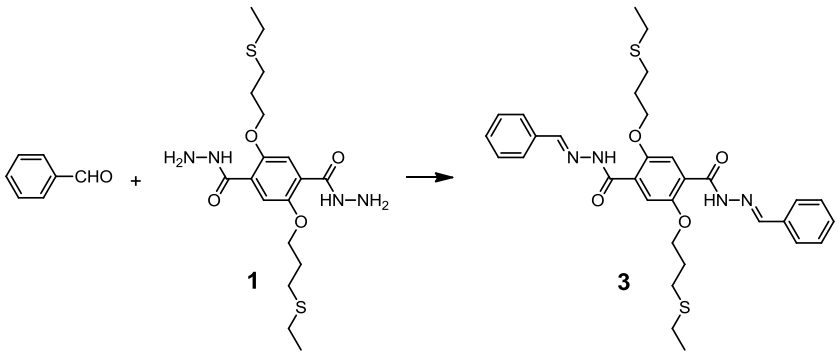

To a solution of 2,5-bis(3-(ethylthio)propoxy)terephthalohydrazide **1** (86 mg,

0.20 mmol) in MeOH (10 mL), benzaldehyde (45 μL, 0.44 mmol) was added at room temperature. The mixture was refluxed for 48 h, and white solids were precipitated. The solid was isolated by sucking filtration, washed with MeOH, dried at 80 ºC under vacuum for 12 h to yield **3** as a white powder (103 mg, 85% yield). **^{1}H NMR** (400 MHz, DMSO-d_6) (major isomer): δ = 11.56 (s, 2H), 8.30 (s, 2H), 7.73−7.70 (m, 4H), 7.49−7.27 (m, 6H), 7.37 (s, 2H), 4.18−4.11 (m, 4H), 2.66−-2.61 (m, 4H), 2.45−2.39 (m, 4H), 2.01−1.95 (m, 4H), 1.11−1.05 (m, 6H). **^{13}C NMR** (100 MHz, DMSO-d_6) (major isomer): δ = 161.9, 150.2, 147.9, 134.7, 130.6, 129.3, 127.5, 127.1, 115.2, 68.5, 29.3, 27.4, 25.3, 15.1. **ESI-HRMS**: calcd. for [$C_{32}H_{38}N_4O_4S_2$ + Na] 629.2334, found 629.2227.

D. FT-IR Spectra

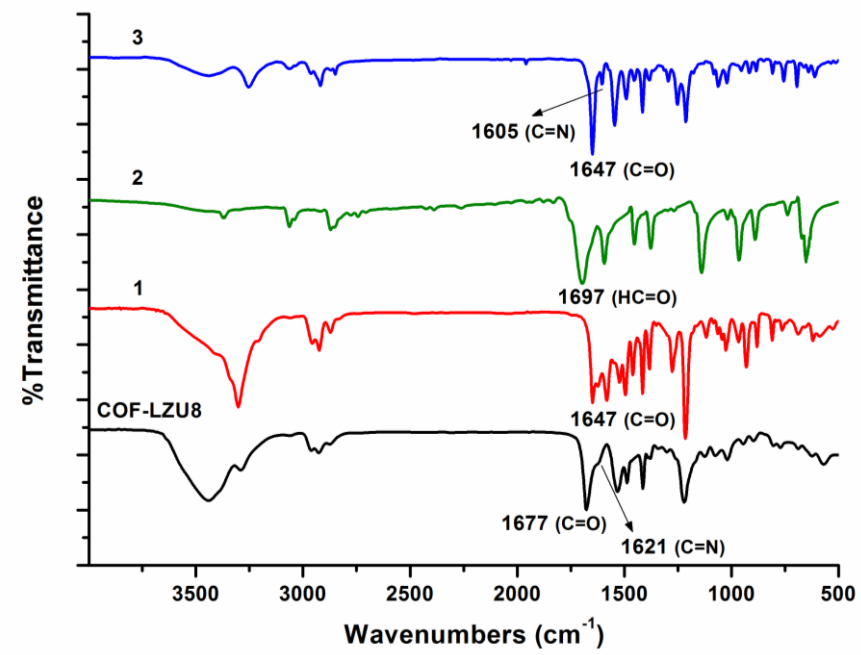

Figure S1. FT-IR spectra of COF-LZU8 (black), the monomer 2,5-bis(3-(ethylthio)-propoxy) terephthalohydrazide **1** (red), the monomer 1,3,5-triformylbenzene **2** (green), and the model compound **3** (blue). In COF-LZU8, the $\nu_{C=O}$ band was observed at 1677 cm^{-1}, which is blue shifted from the corresponding bands (1647 cm^{-1}) of the monomer **1** and the model compound **3**. This blue shift can be attributed to the attenuation of the $\nu_{C=O}$ bonds from the adjacent imine bonds, the situation of which has also been observed in COF-42[6].

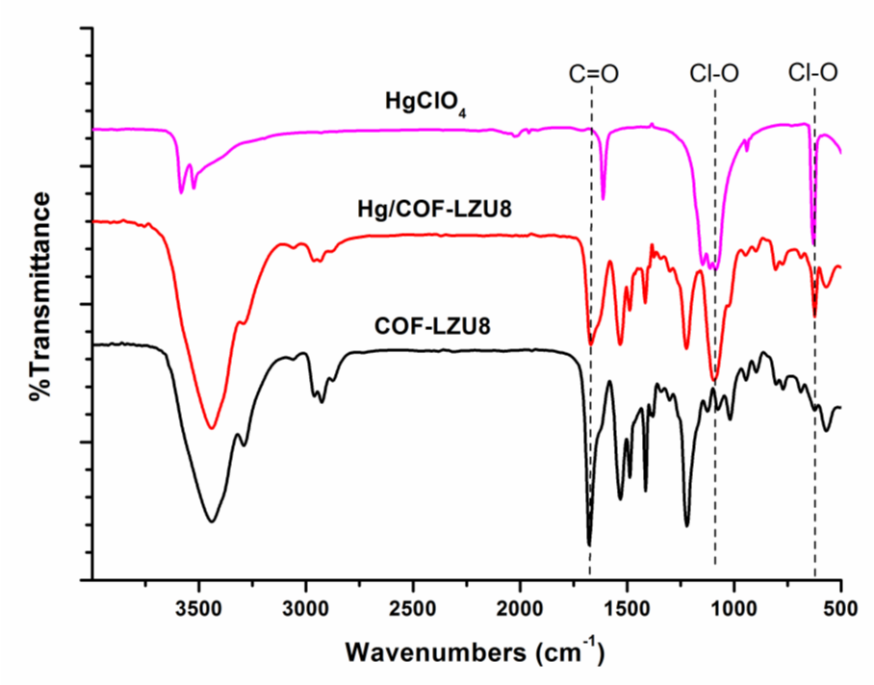

Figure S2. FT-IR spectra of COF-LZU8 (black), Hg/COF-LZU8 (red), and $Hg(ClO_4)_2$ (purple). The $\nu_{C=O}$ band at 1677 cm^{-1} was almost unchanged, implying that Hg^{2+} does not bind to the −C=O bonds (instead, to the S atoms, see the main text) in COF-LZU8.

E. UV/Vis Absorption Spectra

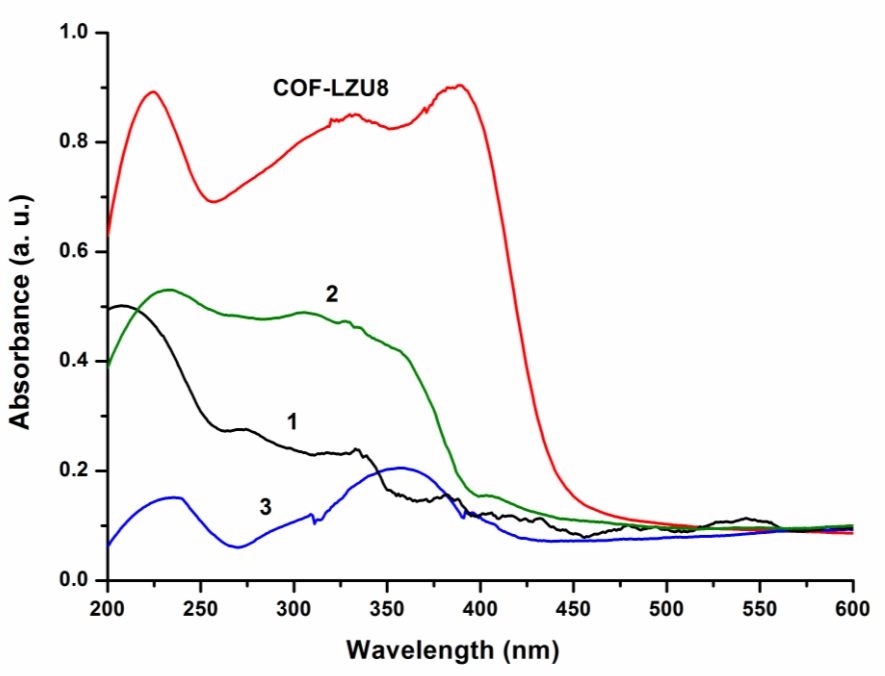

Figure S3. UV/Vis absorption spectra of COF-LZU8 (red), the monomer **2** (green), the monomer **1** (black), and the model compound **3** (blue) in the solid state. COF-LZU8 displays a strong UV absorption band at ~390 nm in the solid state, which is bathochromic from those of its structural monomers (**1**, **2**, and **3**). This difference is attributed to the existence of the extended π-conjugation in the COF-LZU8 framework.

F. Fluorescence Spectra

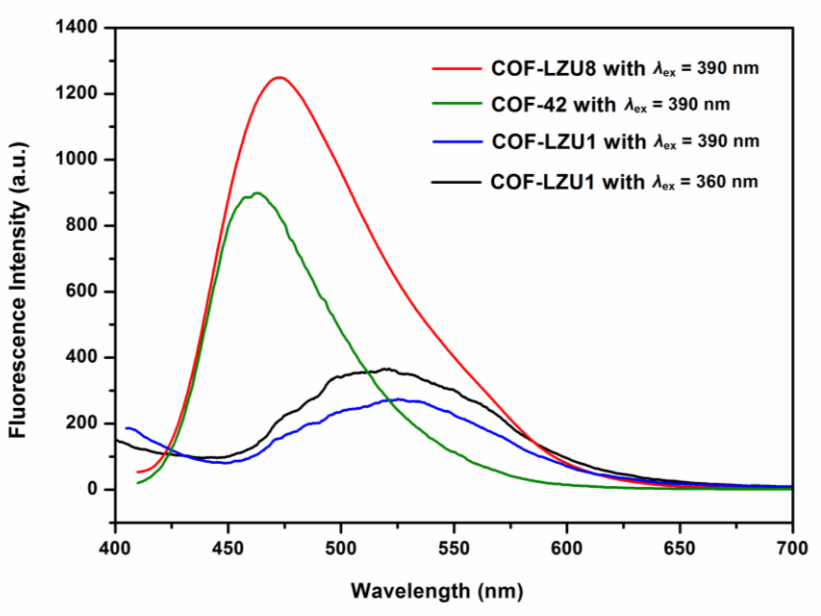

Figure S4. Fluorescence spectra of COF-LZU8 (red), COF-42 (green) and COF-LZU1 (black or blue) in the solid state. In comparison with COF-LZU8, COF-LZU1 shows very weak fluorescence.

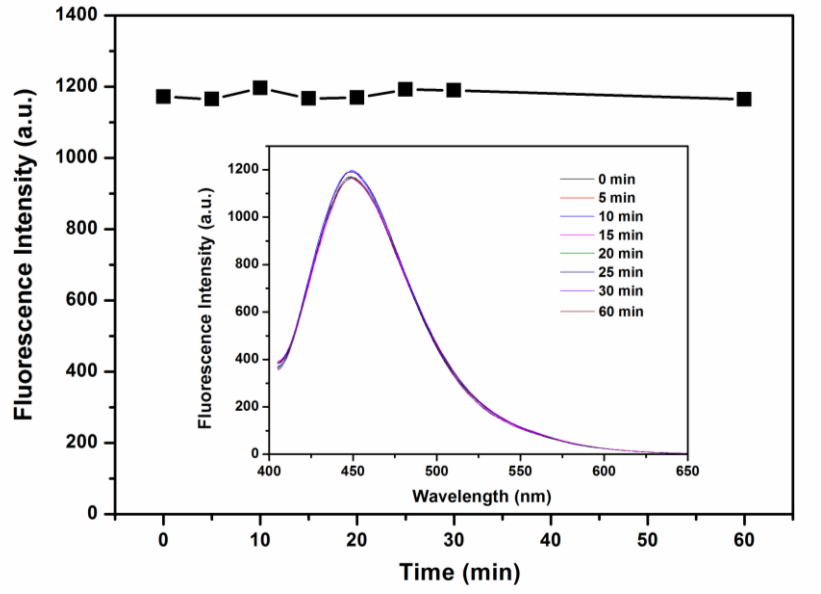

Figure S5. Time-dependent fluorescence intensity of COF-LZU8 (dispersed in acetonitrile) tested within 60 minutes. The unchanged intensity indicates that COF-LZU8 does not show any photo-bleaching, and, the observed decrease in intensities in other cases is indeed induced by the addition of metal ions, such as Hg^{2+}.

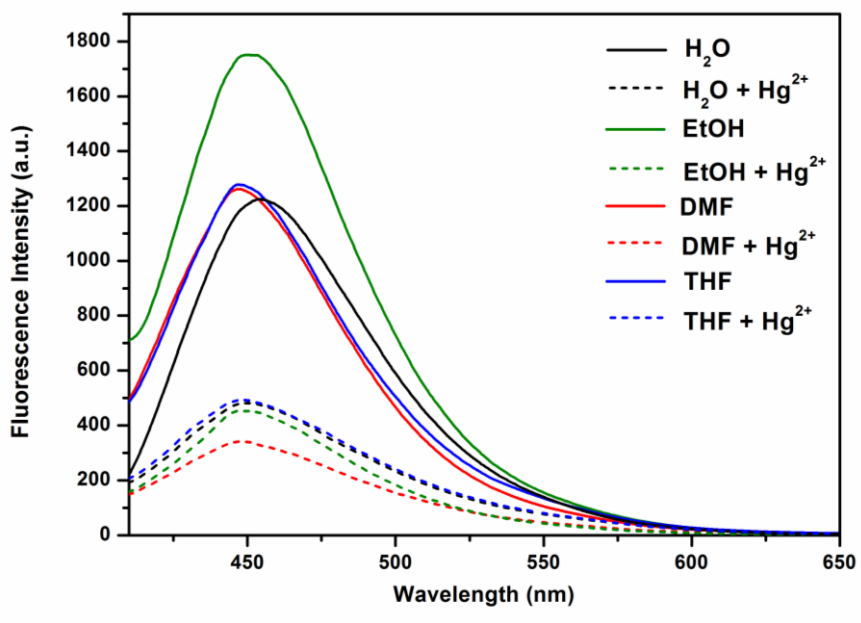

Figure S6. Fluorescence spectra of COF-LZU8 dispersed in H_2O (black), EtOH (green), DMF (red), and THF (blue) before (solid lines) and after (dashed lines) the addition of Hg^{2+} (λ_{ex} = 390 nm).

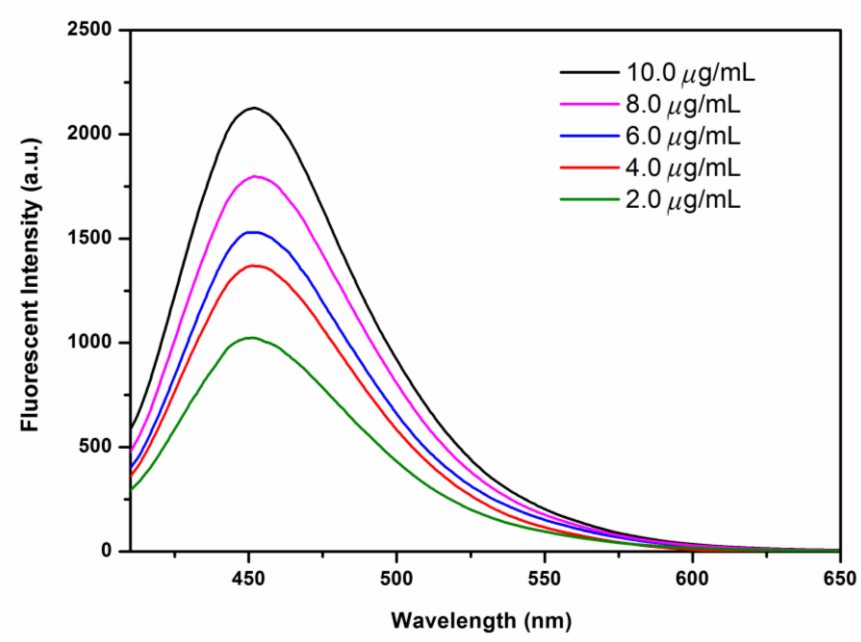

Figure S7. Fluorescence emission intensity against the concentration of COF-LZU8 dispersed in acetonitrile (λ_{ex} = 390 nm).

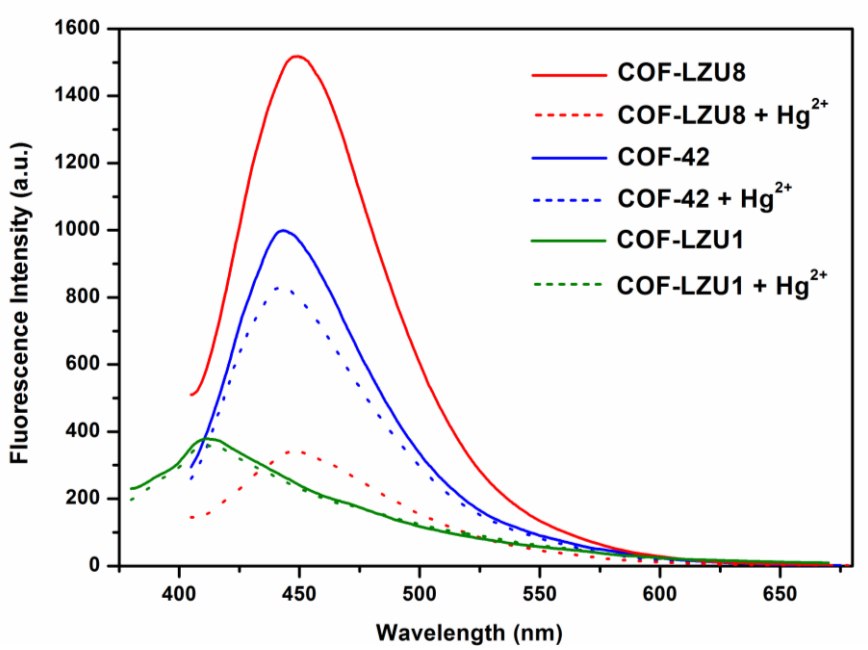

Figure S8. Fluorescence spectra of COF-LZU8 (red), COF-42 (blue), and COF-LZU1 (green) before (solid lines) and after (dashed lines) the addition of Hg^{2+} (1.0 equiv.) in acetonitrile (λ_{ex} = 390 nm). In significant difference from those of COF-LZU1 and COF-42, the effective quenching of the fluorescence in the COF-LZU8 case indicates the unique selectivity of the thioether-based COF-LZU8.

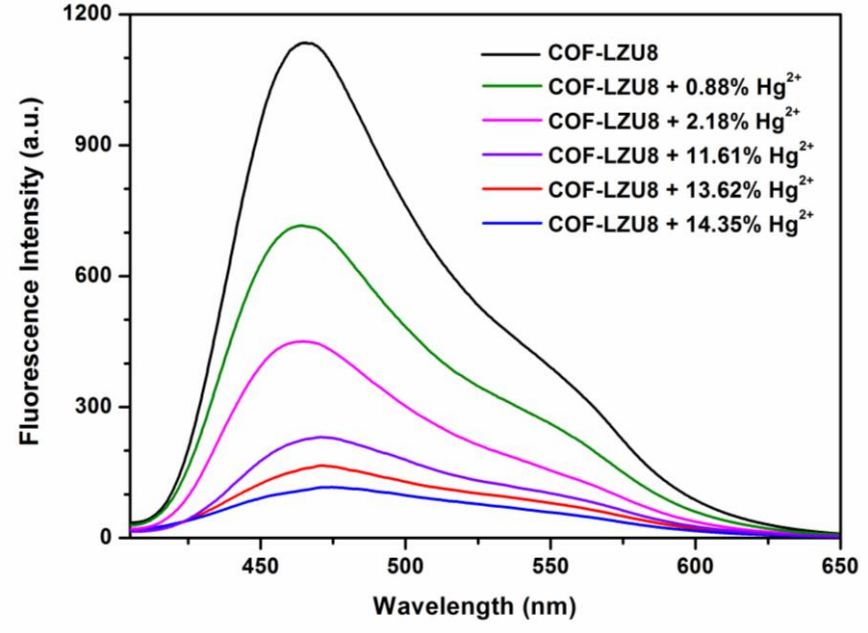

Figure S9. Fluorescence spectra of COF-LZU8 in the solid state (λ_{ex} = 390 nm) upon the addition of Hg^{2+}.

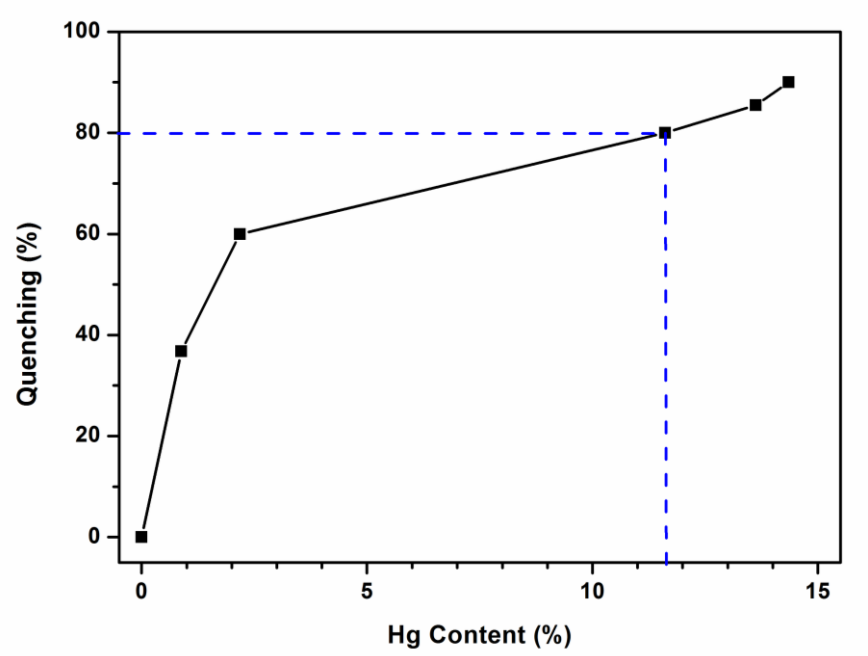

Figure S10. Fluorescence quenching of COF-LZU8 against the Hg^{2+} content in the solid state (λ_{ex} = 390 nm), plotted from the data shown in Figure S9. COF-LZU8 with 11.6% of Hg^{2+} content (corresponding to 1.6 Hg atoms per unit cell) resulted in 80% fluorescence quenching, indicating the amplified fluorescence response of COF-LZU8 in the detection of Hg^{2+}.

G. The Detection Limit of COF-LZU8 with Hg^{2+}

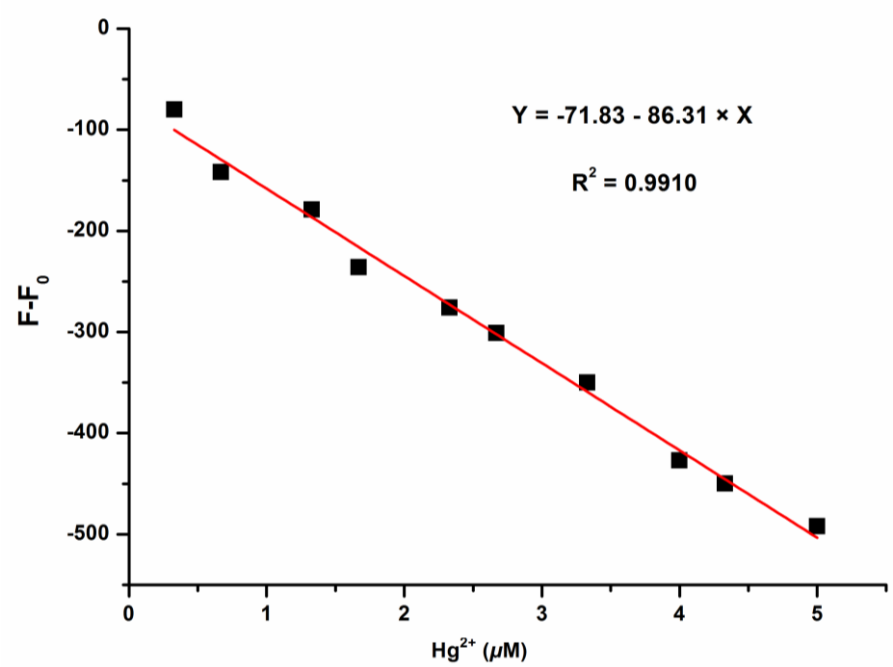

Figure S11. Linear concentration range of Hg^{2+} for COF-LZU8 in acetonitrile (λ_{ex} = 390 nm). The F_0 and F represent the fluorescence emission intensities of COF-LZU8 in the absence and in the presence of Hg^{2+}, respectively. The corresponding limit of detection (LOD) was determined as 25.0 ppb using the equation LOD = 3 × S.D./k,[7] where k represents the slope of the curve equation, and S.D. is the standard deviation for F_0 (the fluorescence intensity of COF-LZU8 in the absence of Hg^{2+}).

H. Structural Modeling and Powder X-Ray Diffraction Analysis

Molecular modeling of COF-LZU8 was generated with the Materials Studio (ver. 6.0) suite of programs. The initial lattice was created by starting with the space group *P*6/*m*; the parameters of $a = b$ = 30.055 Å and c = 3.700 Å were determined by the MS Reflex Plus module. The proposed structure of COF-LZU8 is similar to that of COF-42[6], while the edge of the hexagonal ring was substituted by (N^1E, N^4E)-N^1,N^4-dibenzylidene-2,5-bis(3-(ethylthio)propoxy)terephthalohydrazide, the geometry of which was initially optimized with MS DMol[3] module.

Firstly, we degraded the symmetry of the lattice to *P*1, inserted the optimized monomer in the empty cell, omitted the redundant atoms, and promoted the symmetry to *P*3, producing the crude structure of COF-LZU8. Then the lattice model was geometry-optimized using the MS Forcite molecular dynamics module (universal force fields, Ewald summations) to obtain the optimized lattice parameters of $a = b$ = 29.131 Å and c = 3.703 Å. The optimized structure of COF-LZU8 shows a contorted arrangement, similar to the cyclotricatechylene (CTC) and cyclotriveratrylene (CTV) containing COFs.[8] Finally, Pawley refinement was applied to define the lattice parameters, producing the refined PXRD profile with the lattice parameters of $a = b$ = 29.030 (± 0.466) Å and c = 3.667 (± 0.057) Å. The *wR*p and *R*p values converged to 8.20 % and 6.80 %, respectively (line broadening from the crystallite size and lattice strain were both concerned). A staggered arrangement for COF-LZU8 was constructed wherein the alternating stacked units were offset by *a*/2 and *b*/2 (see Figure S13).

Table S1. Fractional atomic coordinates for the unit cell of COF-LZU8.

COF-LZU8: Space group symmetry *P*3 *a* = *b* = 29.131 Å *c* = 3.703 Å alpha = beta = 90º gamma = 120º			
Atom	*x* (Å)	*y* (Å)	*z* (Å)
C1	0.28258	−0.85350	0.54982
C2	0.29629	−0.89304	0.49543
C3	0.34700	−0.87987	0.61474
C4	0.38562	−0.82689	0.70955
C5	0.37106	−0.78793	0.77136
C6	0.31849	−0.80468	0.71878
O7	0.40949	−0.73200	0.77293
C8	0.40048	−0.69050	0.90239
C9	0.44787	−0.63415	0.79601
C10	0.42953	−0.59249	0.80231
S11	0.48107	−0.52571	0.65301
C12	0.43672	−0.50026	0.51523
C13	0.46882	−0.44442	0.35032
O14	0.26179	−0.94228	0.31208
C15	0.27468	−0.98409	0.32481
C16	0.22538	−1.03723	0.22463
C17	0.23717	−1.08276	0.16038
S18	0.17755	−1.14649	0.23756
C19	0.20747	−1.18832	0.19797
C20	0.16719	−1.24473	0.32397
C21	0.44010	−0.81276	0.63322
N22	0.48127	−0.76189	0.63959
O23	0.44729	−0.84621	0.48489
N24	0.52597	−0.74654	0.42527
C25	0.56272	−0.69743	0.40008
C26	0.61182	−0.68327	0.21245
C27	0.62714	−0.72110	0.18264
C28	0.23047	−0.86077	0.47306
O29	0.22310	−0.82422	0.55073
N30	0.18724	−0.90889	0.40267
N31	0.13907	−0.92155	0.56076
C32	0.10550	−0.96997	0.64745
C33	0.05481	−0.98319	0.80567
C34	0.03920	−0.94545	0.83466
H35	0.35942	−0.90902	0.58345
H36	0.30654	−0.77709	0.79477

H37	0.39702	−0.69394	1.19732
H38	0.36260	−0.69444	0.79923
H39	0.46307	−0.63525	0.52321
H40	0.48466	−0.61987	0.96914
H41	0.41844	−0.58969	1.08152
H42	0.39212	−0.60583	0.64888
H43	0.41033	−0.50173	0.73890
H44	0.40884	−0.52642	0.30463
H45	0.49865	−0.44515	0.16613
H46	0.48933	−0.41481	0.56493
H47	0.44169	−0.43480	0.19750
H48	0.28865	−0.98784	0.59514
H49	0.30844	−0.97441	0.14188
H50	0.20769	−1.03122	−0.01965
H51	0.19343	−1.04885	0.42988
H52	0.26986	−1.08018	0.33012
H53	0.24945	−1.08248	−0.12108
H54	0.24557	−1.17160	0.35262
H55	0.21863	−1.18916	−0.08528
H56	0.18887	−1.26295	0.45605
H57	0.13865	−1.27093	0.10945
H58	0.13970	−1.24374	0.53588
H59	0.48077	−0.73456	0.81520
H60	0.55983	−0.66701	0.54578
H61	0.59765	−0.76238	0.21115
H62	0.19066	−0.93864	0.27340
H63	0.11416	−1.00167	0.59811
H64	0.06755	−0.90363	0.82305

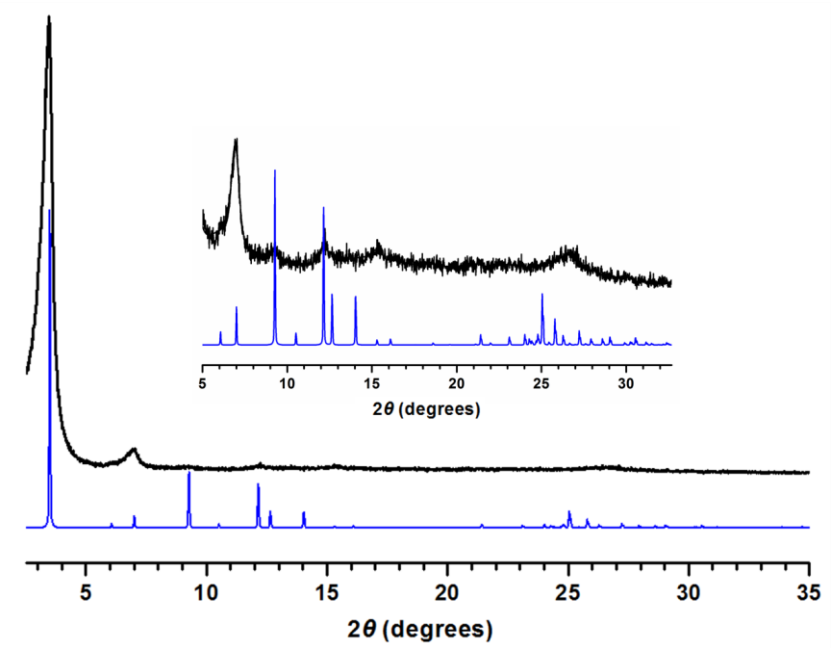

Figure S12. PXRD patterns of COF-LZU8: observed (black) and calculated (blue) with the eclipsed stacking structure. (Inset) Expansion of observed (black) and calculated (blue) PXRD profiles.

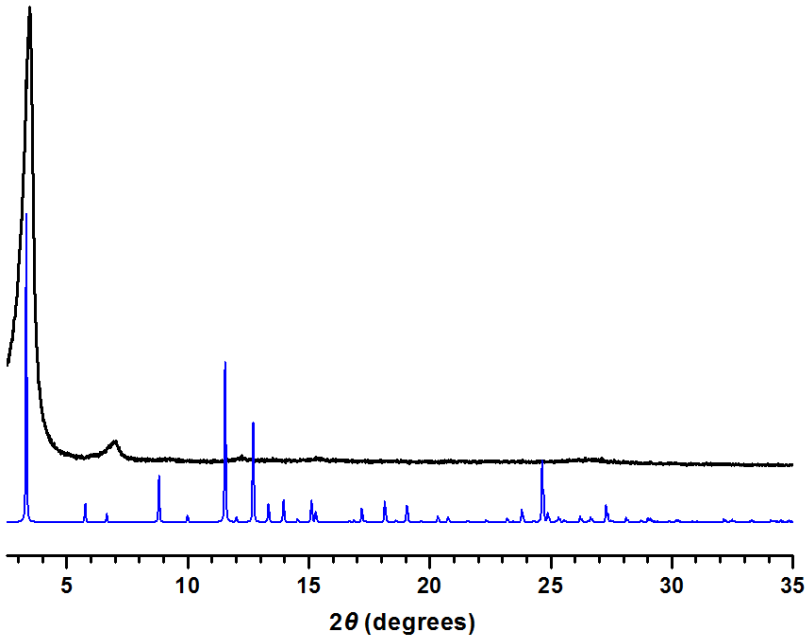

Figure S13. PXRD patterns of COF-LZU8: observed (black) and calculated (blue) with the staggered stacking structure.

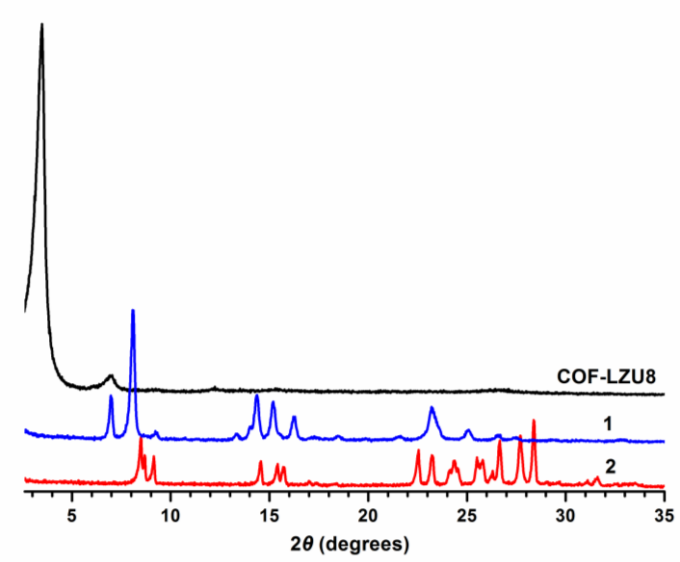

Figure S14. PXRD patterns of COF-LZU8 (black), the monomer **1** (blue), and the monomer **2** (red).

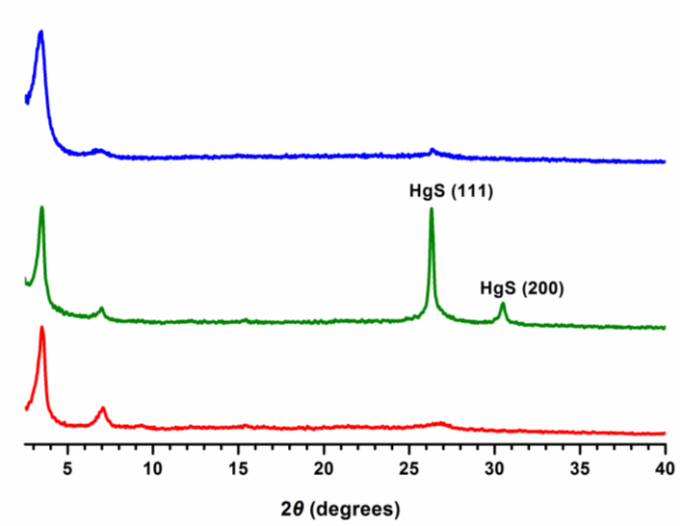

Figure S15. PXRD patterns of COF-LZU8 (red) and the recycled COF-LZU8 after the treatment with 1.0 equiv. (green) and 10.0 equiv. (blue) of aqueous Na_2S solution. It can be seen that the COF-LZU8 crystalline structure was well preserved after the recycle use. Two additional peaks, corresponding to the (111) and (200) facets of HgS, appeared (green) in the PXRD patterns of the recycled COF-LZU8 after the treatment with 1.0 equiv. of aqueous Na_2S solution, indicating the successful deposition of Hg^{2+} via the addition of Na_2S. Upon further addition of aqueous Na_2S solution (10.0 equiv.), the HgS peaks disappeared (blue): the insoluble HgS was easily removed via the formation of soluble $[HgS_2]^{2-}$ complex upon the addition of excess Na_2S solution.[3c, 3d]

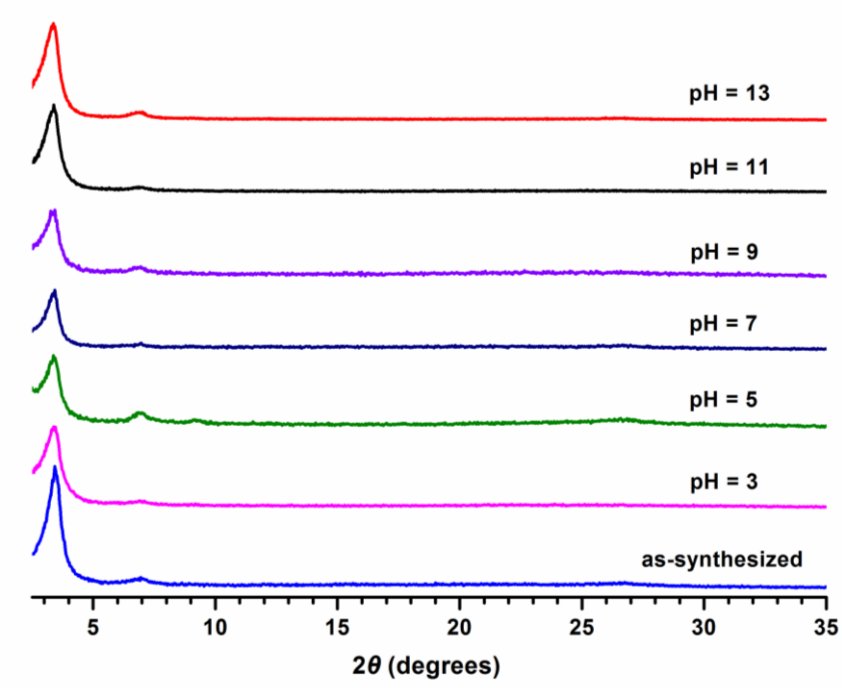

Figure S16. PXRD patterns of COF-LZU8 before and after the treatment in aqueous solutions with different pH values from 3 to 13. The PXRD patterns of COF-LZU8 are preserved in these conditions, indicating its remarkable stability.

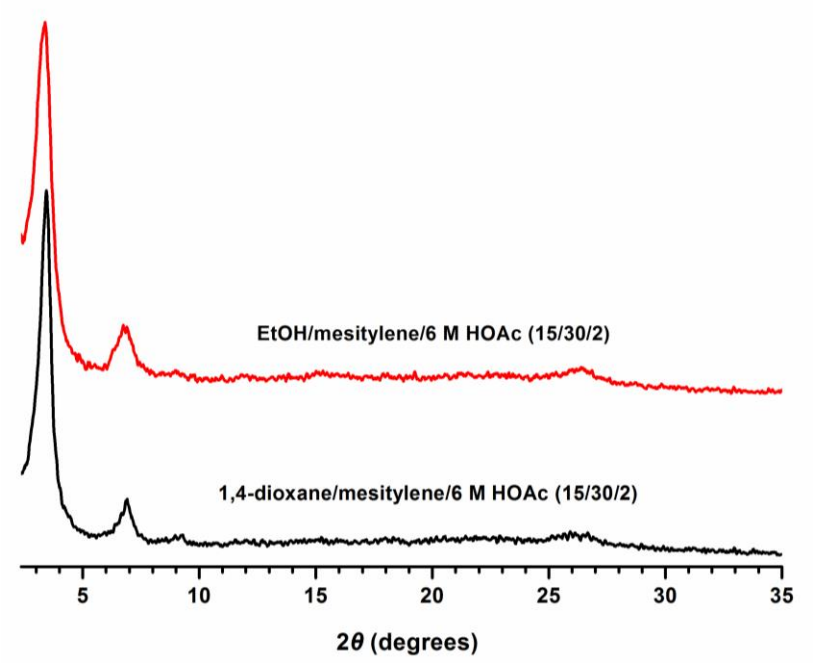

Figure S17. PXRD patterns of COF-LZU8 synthesized under other conditions, such as in 1,4-dioxane/mesitylene/6.0 M HOAc (15/30/2) (black) or in EtOH/mesitylene/ 6.0 M HOAc (15/30/2) (red).

I. N_2 Adsorption-Desorption Analysis

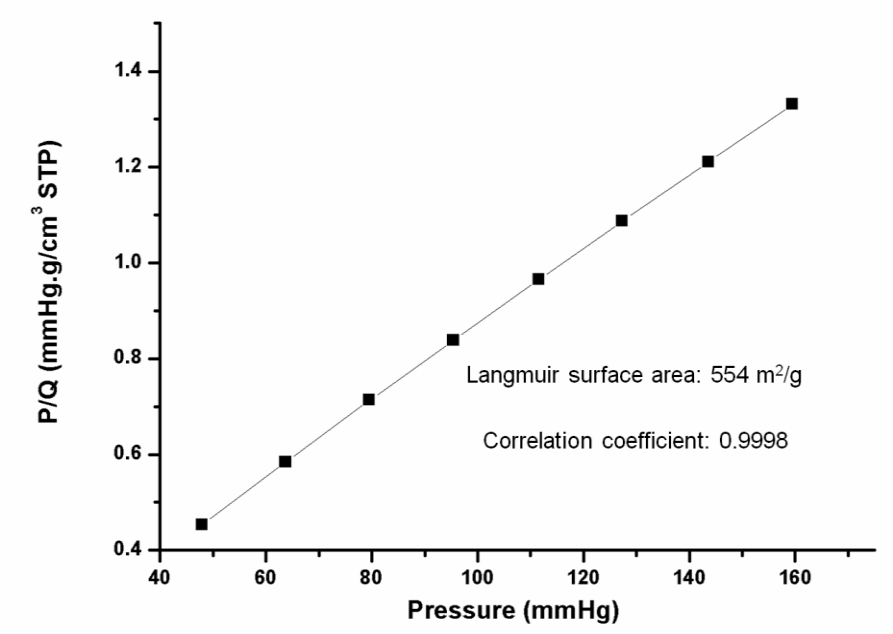

Figure S18. Langmuir surface area plot for COF-LZU8 calculated from the isotherm.

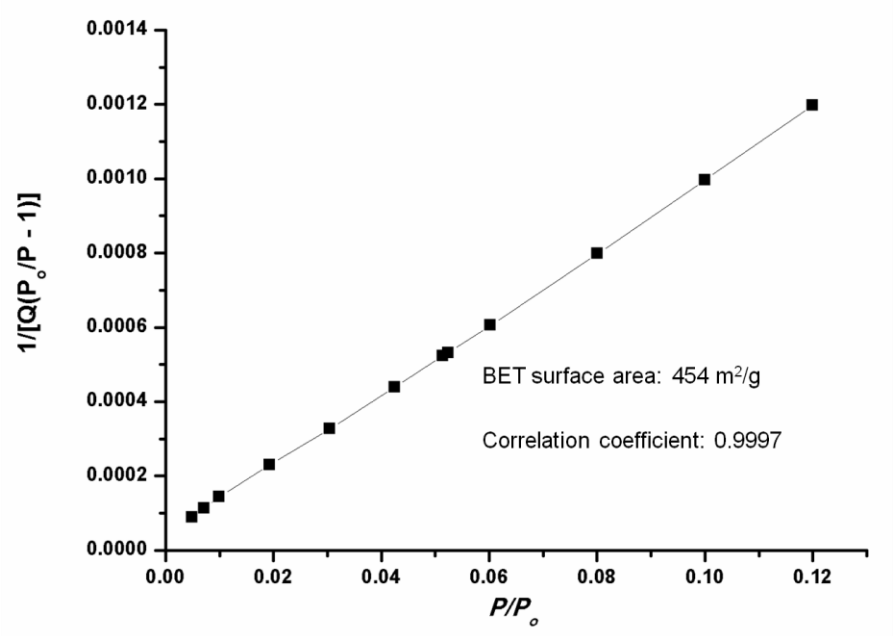

Figure S19. BET surface area plot for COF-LZU8 calculated from the isotherm.

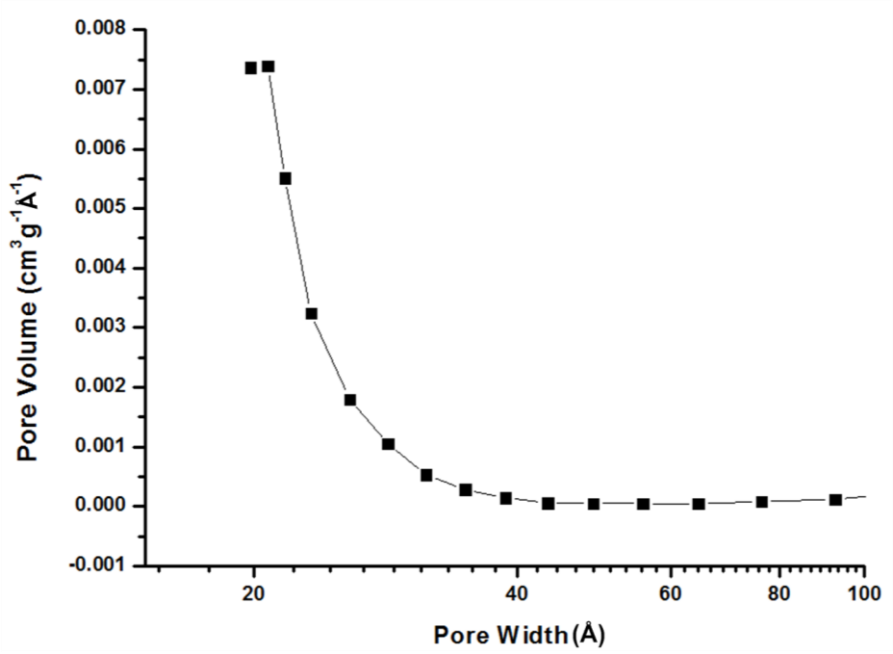

Figure S20. Pore size distribution of COF-LZU8 calculated by the BJH method based on the adsorption isothermal.

J. Thermogravimetric Analysis

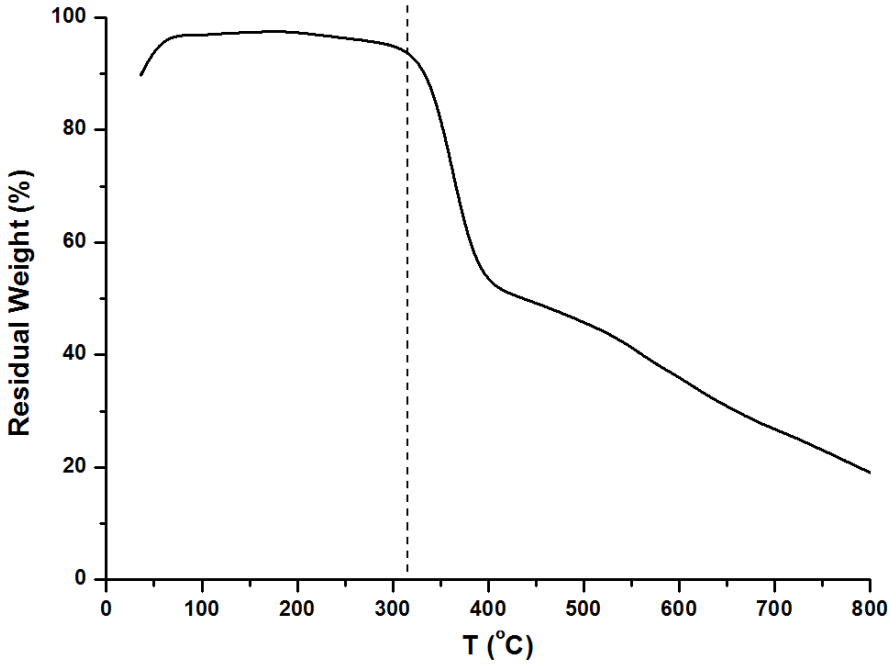

Figure S21. TGA data for COF-LZU8.

K. Scanning Electron Micrographs

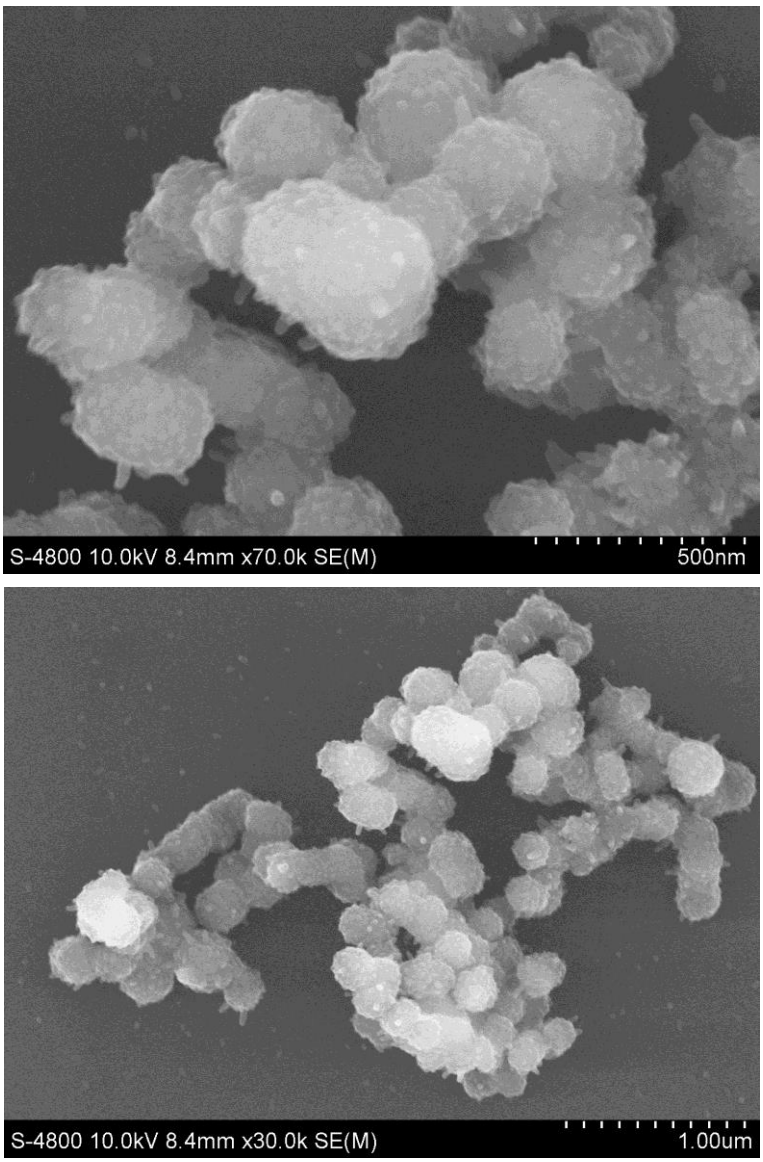

Figure S22. SEM images of COF-LZU8.

L. Liquid NMR Spectra

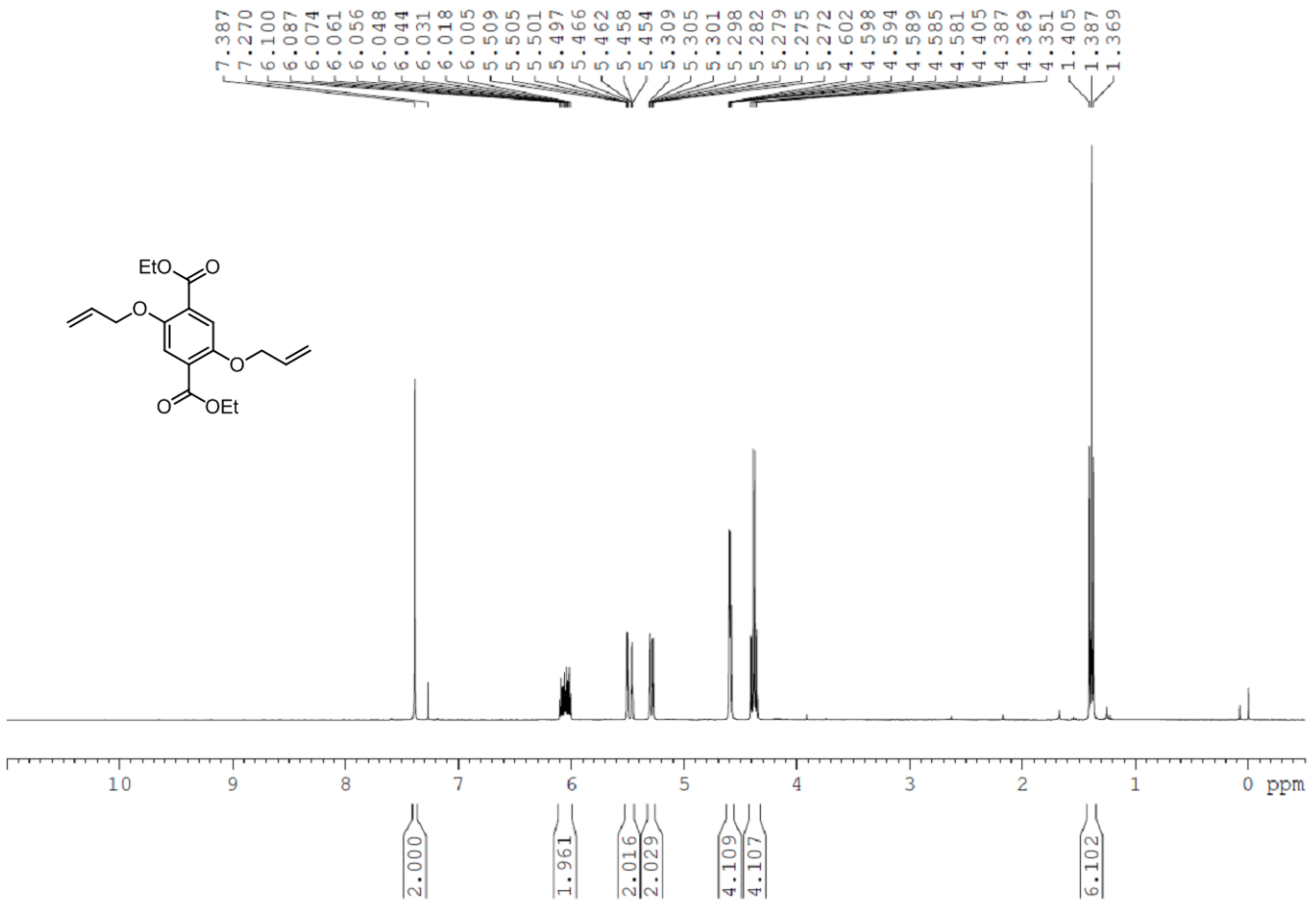

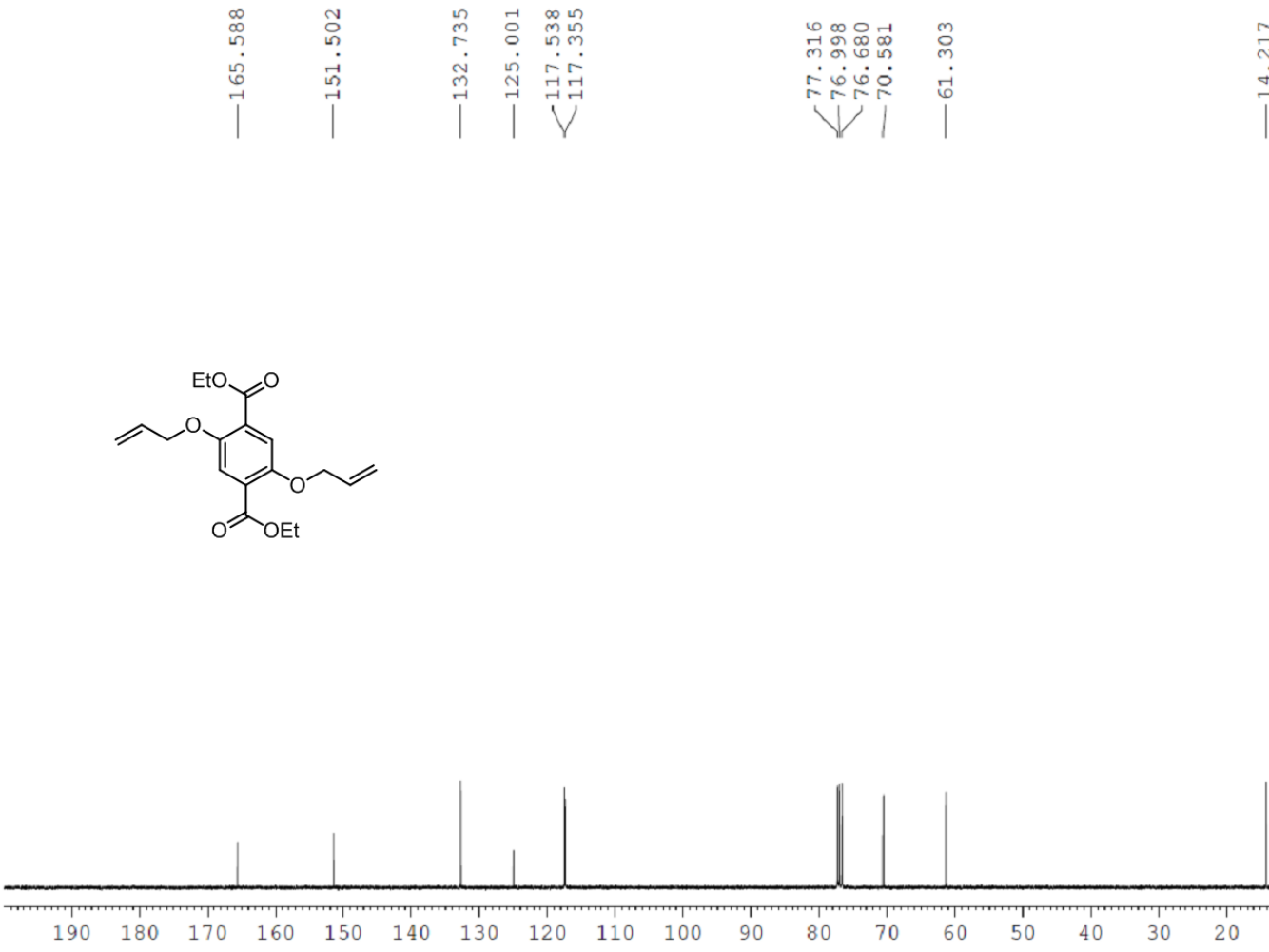
165.588
151.502
132.735
125.001
117.538
117.355
77.316
76.998
76.680
70.581
61.303
14.217
EtO
O
O
O
O
OEt
190 180 170 160 150 140 130 120 110 100 90 80 70 60 50 40 30 20 10 ppm

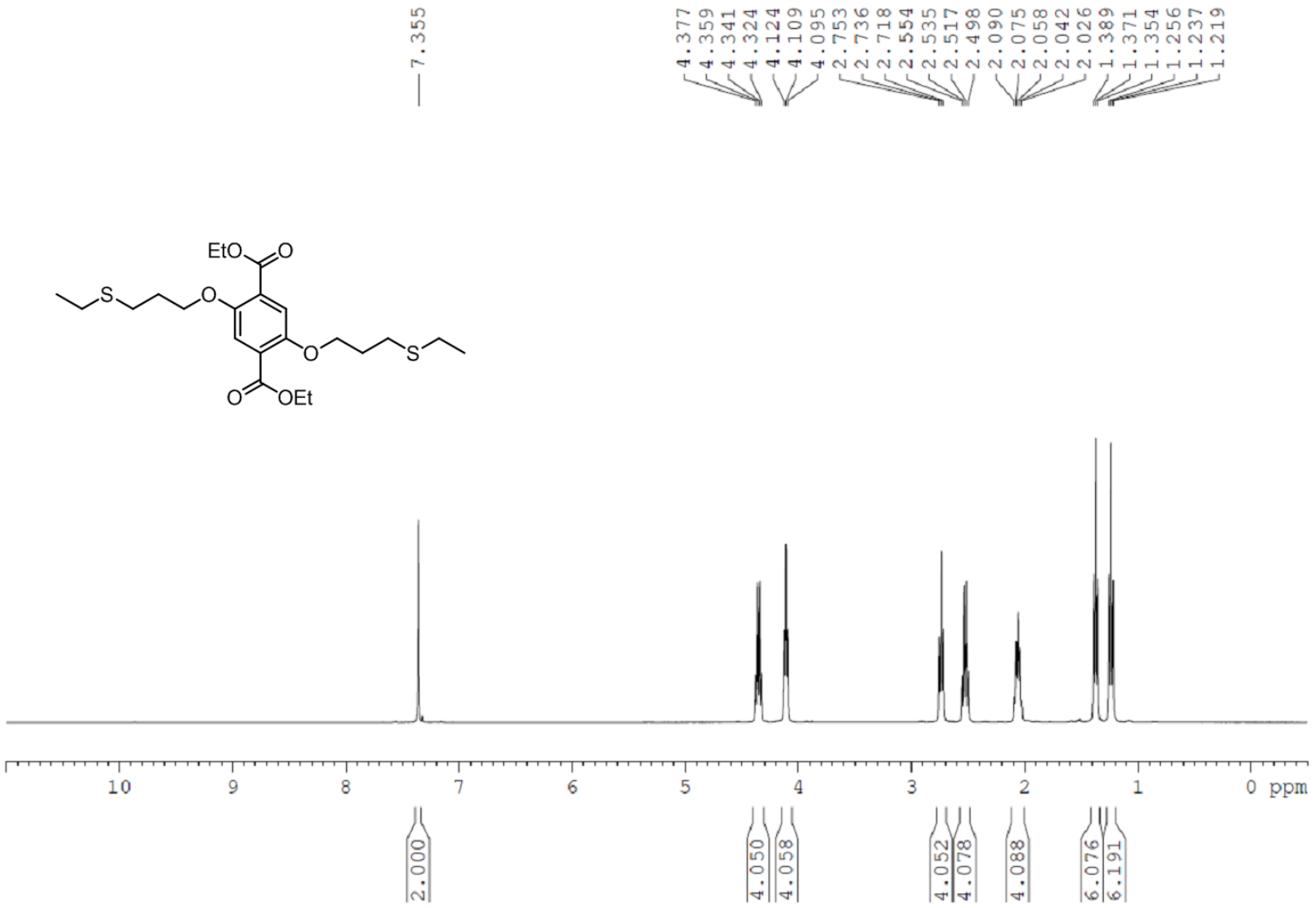
7.355
4.377
4.359
4.341
4.324
4.124
4.109
4.095
2.753
2.736
2.718
2.554
2.535
2.517
2.498
2.090
2.075
2.058
2.042
2.026
1.389
1.371
1.354
1.256
1.237
1.219
EtO
O
S
O
O
S
O
OEt
10
9
8
7
6
5
4
3
2
1
0 ppm
2.000
4.050
4.058
4.052
4.078
4.088
6.076
6.191

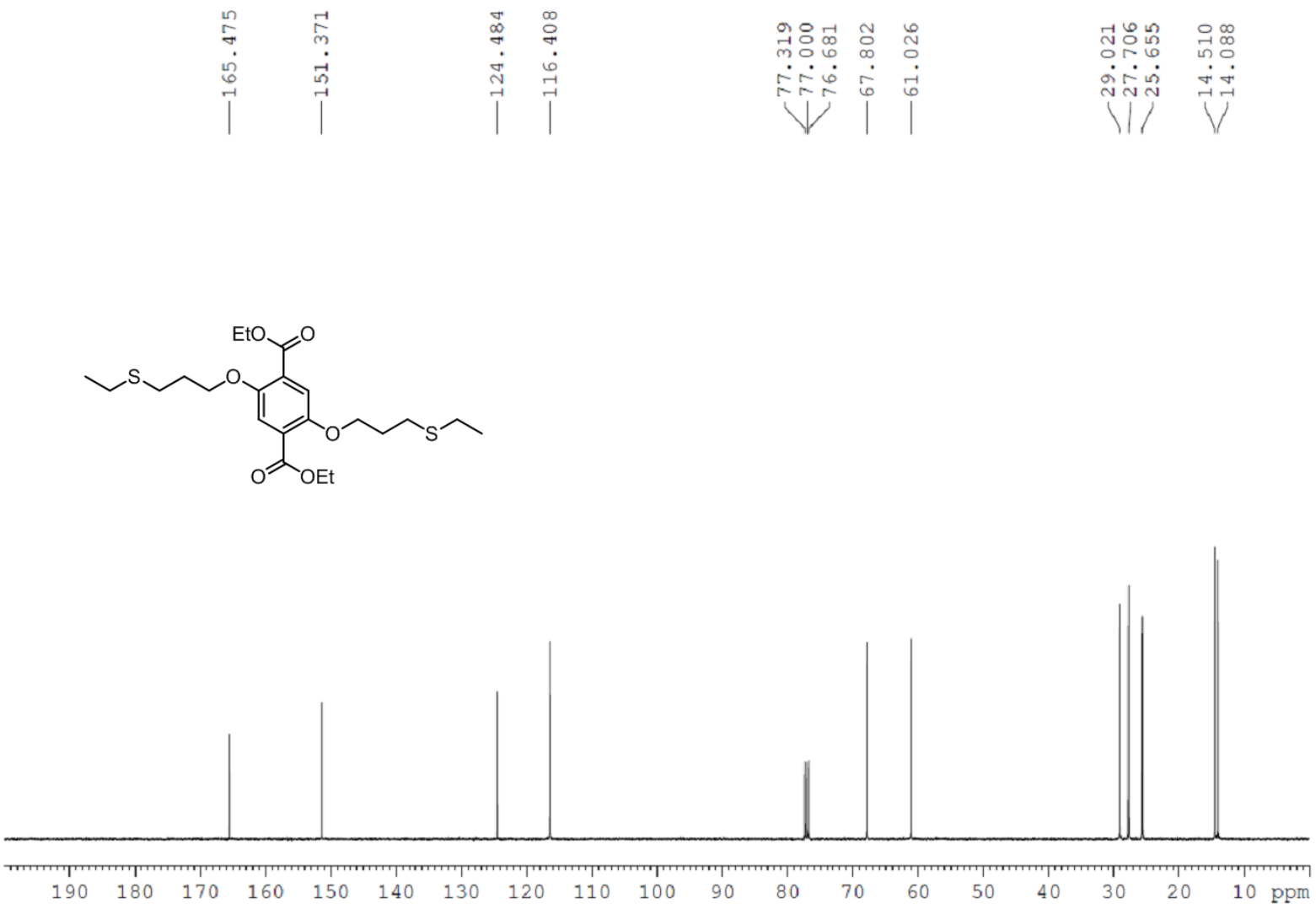
165.475
151.371
124.484
116.408
77.319
77.000
76.681
67.802
61.026
29.021
27.706
25.655
14.510
14.088
EtO
O
S
O
O
S
O
OEt
190 180 170 160 150 140 130 120 110 100 90 80 70 60 50 40 30 20 10 ppm

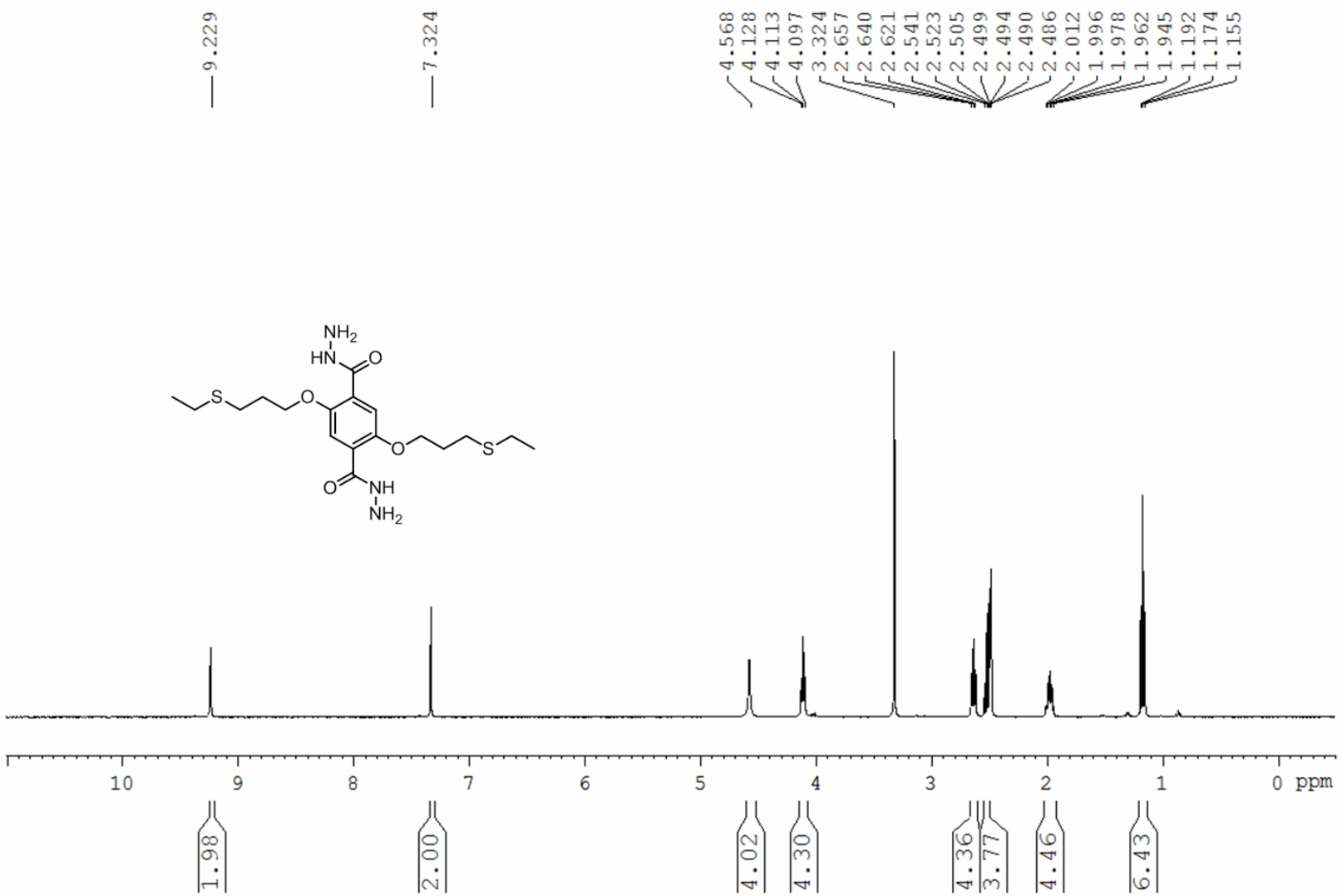
9.229
7.324
4.568
4.128
4.113
4.097
3.324
2.657
2.640
2.621
2.541
2.523
2.505
2.499
2.494
2.490
2.486
2.012
1.996
1.978
1.962
1.945
1.192
1.174
1.155
NH2
HN
O
S
O
O
S
O
NH
NH2
10
9
8
7
6
5
4
3
2
1
0 ppm
1.98
2.00
4.02
4.30
4.36
3.77
4.46
6.43

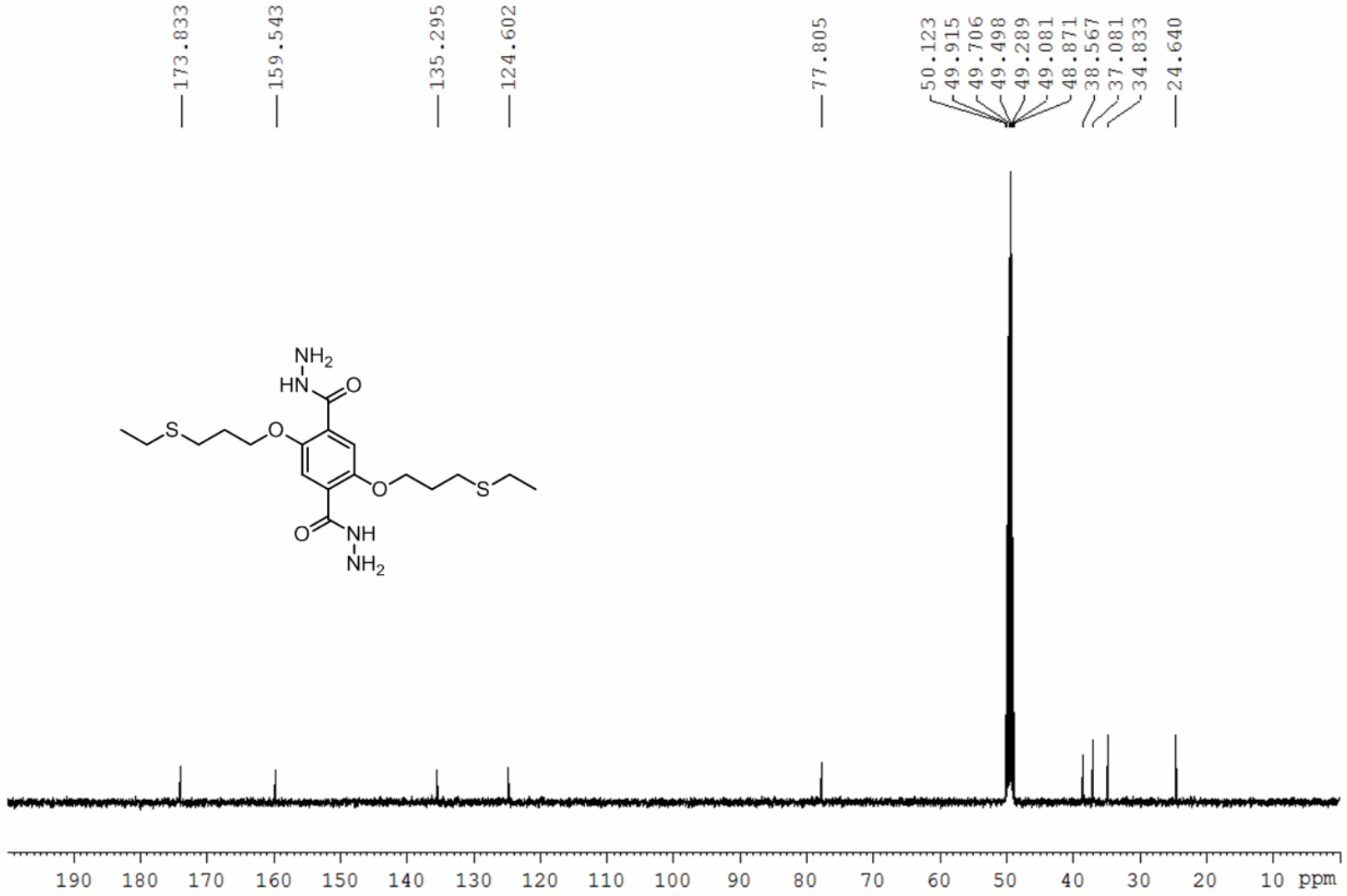
173.833
159.543
135.295
124.602
77.805
50.123
49.915
49.706
49.498
49.289
49.081
48.871
38.567
37.081
34.833
24.640
NH2
HN
O
S
O
O
S
O
NH
NH2
190 180 170 160 150 140 130 120 110 100 90 80 70 60 50 40 30 20 10 ppm

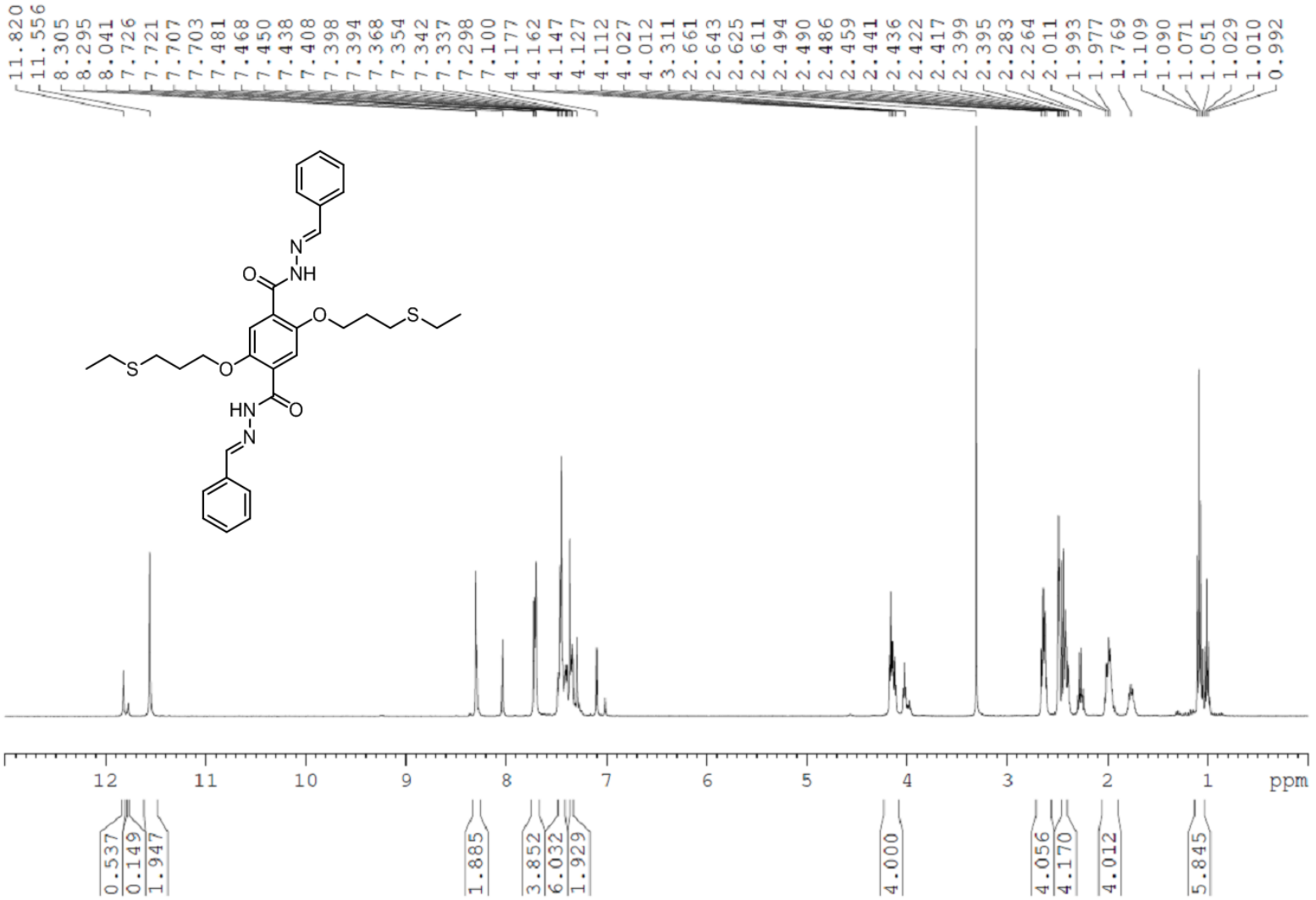
11.820
11.556
8.305
8.295
8.041
7.726
7.721
7.707
7.703
7.481
7.468
7.450
7.438
7.408
7.398
7.394
7.368
7.354
7.342
7.337
7.298
7.100
4.177
4.162
4.147
4.127
4.112
4.027
4.012
3.311
2.661
2.643
2.625
2.611
2.494
2.490
2.486
2.459
2.441
2.436
2.422
2.417
2.399
2.395
2.283
2.264
2.011
1.993
1.977
1.769
1.109
1.090
1.071
1.051
1.029
1.010
0.992
N
NH
O
O
S
O
S
HN
O
N
12
11
10
9
8
7
6
5
4
3
2
1
ppm
0.537
0.149
1.947
1.885
3.852
6.032
1.929
4.000
4.056
4.170
4.012
5.845

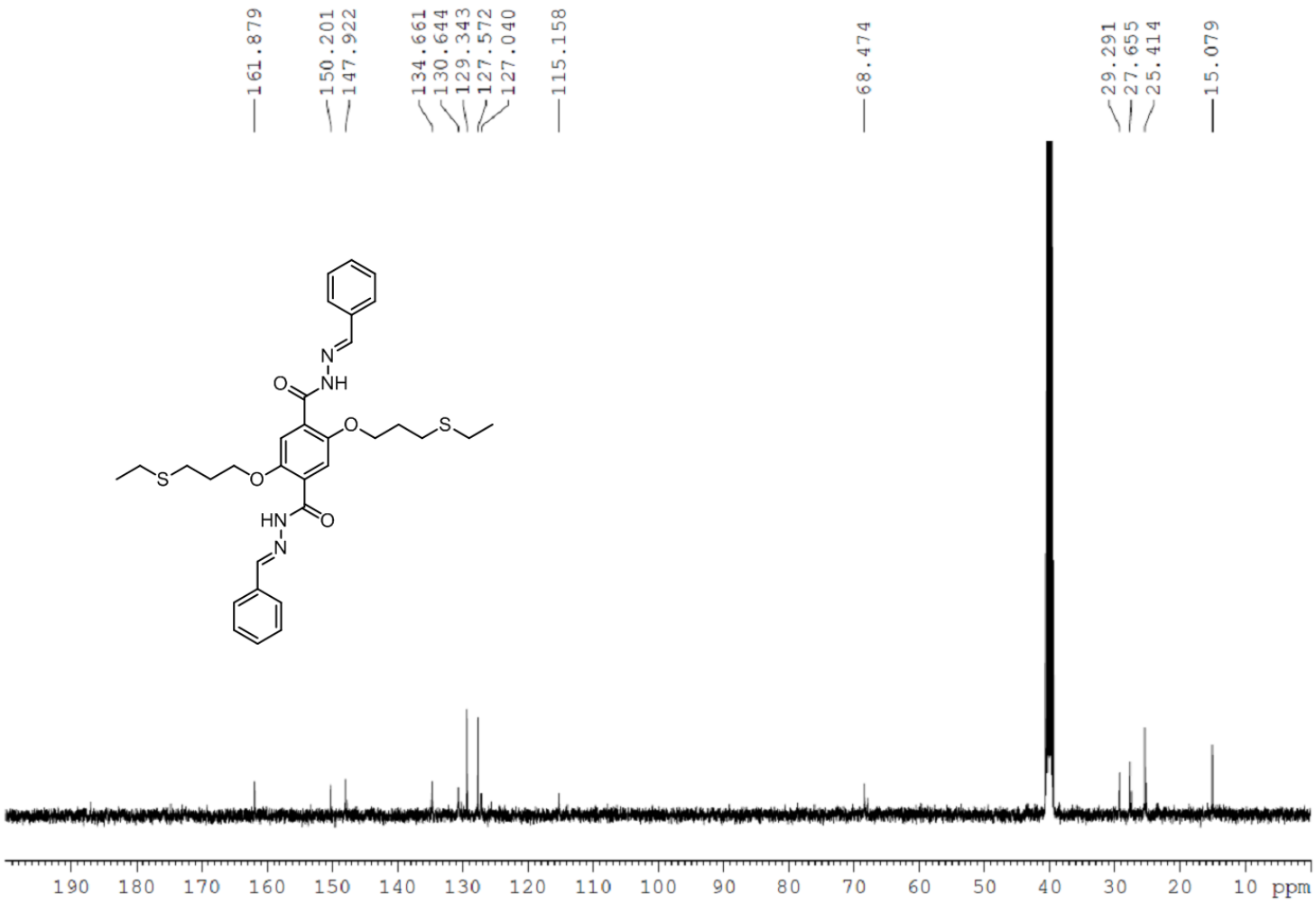
161.879
150.201
147.922
134.661
130.644
129.343
127.572
127.040
115.158
68.474
29.291
27.655
25.414
15.079
190 180 170 160 150 140 130 120 110 100 90 80 70 60 50 40 30 20 10 ppm

M. References

1. Wrighton, M. S.; Ginley, D. S.; Morse, D. L., *J. Phys. Chem.* **1974**, *78*, 2229.
2. (a) Gole, B.; Bar, A. K.; Mukherjee, P. S., *Chem. Commun.* **2011**, *47*, 12137; (b) Sun, L.; Liang, Z.; Yu, J.; Xu, R., *Polym. Chem.* **2013**, *4*, 1932.
3. (a) Wu, D.; Huang, W.; Lin, Z.; Duan, C.; He, C.; Wu, S.; Wang, D., *Inorg. Chem.* **2008**, *47*, 7190; (b) Armstrong, R. D.; Porter, D. F.; Thirsk, H. R., *J. Phys. Chem.* **1968**, *72*, 2300; (c) Findlay, D. M.; McLean, R. A. N., *Environ. Sci. Technol.* **1981**, *15*, 1388; (d) Zhou, Y.; Zhu, C.-Y.; Gao, X.-S.; You, X.-Y.; Yao, C., *Org. Lett.* **2010**, *12*, 2566.
4. Itami, K.; Palmgren, A.; Thorarensen, A.; Bäckvall, J.-E., *J. Org. Chem.* **1998**, *63*, 6466.
5. Ding, S.-Y.; Gao, J.; Wang, Q.; Zhang, Y.; Song, W.-G.; Su, C.-Y.; Wang, W., *J. Am. Chem. Soc.* **2011**, *133*, 19816.
6. Uribe-Romo, F. J.; Doonan, C. J.; Furukawa, H.; Oisaki, K.; Yaghi, O. M., *J. Am. Chem. Soc.* **2011**, *133*, 11478.
7. (a) Long, G. L.; Winefordner, J. D., *Anal. Chem.* **1983**, *55*, 712A; (b) Hussain, S.; De, S.; Iyer, P. K., *ACS Appl. Mater. & Interfaces* **2013**, *5*, 2234.
8. (a) Song, J.-R.; Sun, J.; Liu, J.; Huang, Z.-T.; Zheng, Q.-Y., *Chem. Commun.* **2014**, *50*, 788; (b) Yu, J.-T.; Chen, Z.; Sun, J.; Huang, Z.-T.; Zheng, Q.-Y., *J. Mater. Chem.* **2012**, *22*, 5369.